

ADVANCED FUNCTIONAL MATERIALS

Supporting Information

for *Adv. Funct. Mater.*, DOI: 10.1002/adfm.201704919

Polydimethylsiloxane Composites for Optical Ultrasound Generation and Multimodality Imaging

*Sacha Noimark, Richard J. Colchester, Radhika K. Poduval,
Efthymios Maneas, Erwin J. Alles, Tianrui Zhao, Edward
Z. Zhang, Michael Ashworth, Elena Tsolaki, Adrian H.
Chester, Najma Latif, Sergio Bertazzo, Anna L. David,
Sebastien Ourselin, Paul C. Beard, Ivan P. Parkin, Ioannis
Papakonstantinou, and Adrien E. Desjardins**

Polydimethylsiloxane composites for optical ultrasound generation and multi-modality imaging

Supporting Information

Sacha Noimark, Richard J. Colchester, Radhika K. Poduval, Efthymios Maneas, Erwin J. Alles, Tianrui Zhao, Edward Z. Zhang, Michael Ashworth, Elena Tsolaki, Adrian H. Chester, Najma Latif, Sergio Bertazzo, Anna L. David, Sebastien Ourselin, Paul C. Beard, Ivan P. Parkin, Ioannis Papakonstantinou and Adrien E. Desjardins

Supporting Information

1 Composite Fabrication

1.1 Crystal Violet Composite

A selectively optically absorbing coating based on Crystal Violet (CV) was fabricated onto the tip of an optical fibre (core diameter: 200 μm ; Thorlabs, UK) using a two-step top-down dipping method. Firstly, a polydimethylsiloxane (PDMS) layer was deposited using dip-coating methods. A PDMS solution comprising 1 g PDMS : 2 mL xylene was prepared, degassed (5 minutes at 22 $^{\circ}\text{C}$) and optical fibres were dipped into the solution. Secondly, After air-drying (24 hours) the PDMS coated fibres were immersed in a heated CV solution ($0.005 \text{ mol dm}^{-3}$, 85 $^{\circ}\text{C}$) for *ca.* 13 hours to achieve a selectively optically absorbing CV-PDMS composite.

1.2 Gold Particle Composite

The fabrication of a selectively optically absorbing coating based on gold nanoparticles (AuNPs) by a top-down method comprised two main steps: coating of the tip of an optical fibre (diameter: 400 μm ; Ceramoptec, Germany) with PDMS, and subsequent submersion in gold salt. The PDMS (Sylgard 184, Dow Corning, UK) was prepared with a 10:1 base:catalyst ratio and mixed with toluene, in a 1:1 ratio by weight, to reduce the viscosity. The solution was left to degas at 22 $^{\circ}\text{C}$ for 1 hour. This PDMS was applied to the optical fibre tips using dip-coating methods. Subsequently, the PDMS coatings were cured 5 mm above a hotplate at 180 $^{\circ}\text{C}$ for 30 minutes. A solution of gold salt was prepared by adding 0.5% gold(III) chloride trihydrate (Sigma Aldrich, UK) to ethanol by weight. The solution was stirred for 12 hours to ensure full dissolution. The PDMS-coated optical fibre tips were submerged in the gold salt solution for 24 hours resulting in an AuNP-PDMS composite.

2 Materials Characterisation

2.1 Optical Characterisation

The CV-PDMS and AuNP-PDMS composite coated optical fibres were imaged and optically characterised prior to their use as fibre-optic ultrasound generators. Scanning electron microscopy (SEM) of the CV-PDMS and AuNP-PDMS composite coatings on the distal ends of the optical fibres was carried out using secondary electron imaging on a field emission instrument (JSM-6301F, JEOL, Japan) with an acceleration voltage of 5 kV. Side view SEM imaging was performed to determine the thicknesses of the composite coatings. The wavelength-dependent optical absorption was measured between 400 and 1300 nm using a halogen lamp, an integrating sphere, and two spectrometers (Maya2000 Pro & NIRQuest512, Ocean Optics, USA). An uncoated optical fibre was used for reference and a background count was taken for each measurement to remove ambient light and dark counts.

2.2 Ultrasound Characterisation

For ultrasound characterisation, the fibre-optic ultrasound generators were illuminated through the fibre by a Q-switched laser (FQ-500-532, Elforlight, UK) with a wavelength of 532 nm, a pulse length of 10 ns, and a repetition rate of 100 Hz. The laser fluence delivered to the fibre tip was 86.3 mJ/cm² and 55.3 mJ/cm² for the CV-PDMS and AuNP-PDMS composite coatings, respectively. Ultrasound was received using a needle hydrophone with a diameter of 200 µm (Precision Acoustics, UK), with a calibrated sensitivity ranging from 1 to 30 MHz. The hydrophone was mounted on a three-dimensional translation stage, centred on the generated ultrasound beam at a distance of 1.5 mm from the coating.

2.3 Ultrasound Pressure vs. Time

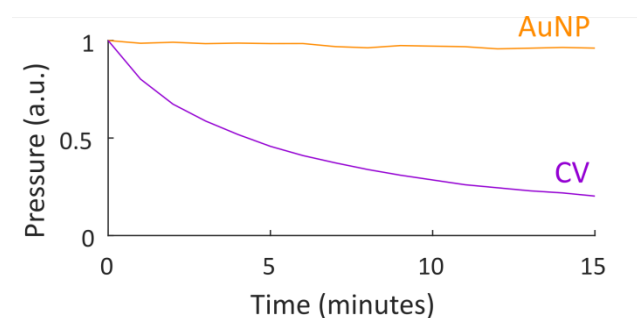


Figure 1: Peak-to-peak ultrasound pressure generated by crystal violet composite (purple line) and AuNP composite (gold line) over an extended time period. The data was normalised to the initial value.

The ultrasound pressure generated by the both the CV and AuNP transmitters was recorded every minute over a period of 15 minutes. For CV-PDMS composite coatings a fluence of 66.8 mJ/cm² was used, whilst for AuNP-PDMS composite coated fibres a fluence of 60.5 mJ/cm² was used. These optical pulse energies were the same as those used to acquire all-optical ultrasound images of *ex vivo* swine abdominal tissue and diseased human aorta. Over the 15 minute time period the pressure generated by the AuNP-PDMS composite remained constant, whereas for the CV-PDMS composite the pressure decreased to 20% of the initial value.

3 All-Optical Ultrasound and Photoacoustic Imaging Setup

For all-optical ultrasound and photoacoustic imaging, the probes, comprising a PDMS composite coated fibre and a Fabry-Pérot fibre-optic sensor were interrogated using a console (Figure 2). For ultrasound reception, the Fabry-Pérot fibre-optic sensor was interrogated using a CW tuneable laser (Tunics T100S CL, Yenista Optics, France) and a power of 1 mW. The laser parameters are summarised in Table 1. For ultrasound generation, pulsed light was coupled into the composite coated fibre. The pulsed light was supplied by one of two sources, the parameters for these are summarised in Table 1. For the 3D human placenta imaging with a multiwalled carbon nanotube (MWCNT) and PDMS composite transmitter, a Q-switched Nd:YAG laser with a wavelength 1064 nm, a pulse length 2 ns, a repetition rate 100 Hz, and a pulse energy of 10 µJ (SPOT-10-500-1064, Elforlight, UK) was used. For the *ex vivo* swine abdominal tissue and *ex vivo* diseased human aorta

imaging with CV-PDMS and AuNP-PDMS composite transmitters, an OPO system with a variable wavelength (450 – 1800 nm), a pulse length 7 ns, a repetition rate 30 Hz, and a variable pulse energy (SpitLight 600, Innolas, UK) was used. For ultrasound generation in CV-PDMS composites, 21 μJ per pulse was used (corresponding fluence: 66.8 mJ/cm^2). For ultrasound generation in AuNP-PDMS composites, 76 μJ per pulse was used (corresponding fluence: 60.5 mJ/cm^2). For photoacoustic imaging, with both composites, 116 μJ per pulse was used. Each ultrasound generator was paired with a fibre-optic ultrasound receiver^[1], and each pair was mounted on a two-dimensional motorised translation stage. Ultrasound imaging was carried out by translating the probe in a single line (2D imaging) or a grid (3D imaging). For 3D placenta imaging, the placenta was placed in a water bath and held in place using metal weights (Figure 3). The scan grid contained 200 x 200 steps at a step size of 100 μm . For 2D ultrasound/ photoacoustic imaging, swine abdominal tissue as well as human aorta tissue were used. All samples were collected under approved ethical guide lines with informed consent that allowed us to anonymously analyse the tissues. The tissue samples used for 2D imaging were pinned to a mount made of cork which was fixed on a metal base. A step size of 25 μm and 1800 steps were used and each A-line was averaged 10 times.

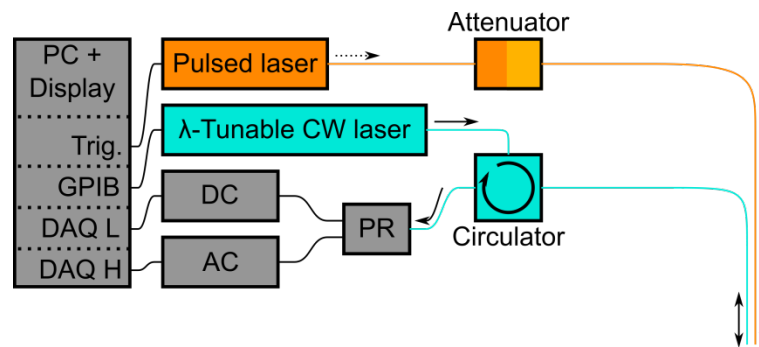


Figure 2: All-optical ultrasound imaging console schematic. Pulsed light is delivered for ultrasound generation via an attenuator. CW wavelength (λ) tuneable light is delivered via a circulator for reception. Reflected light is detected with a photoreceiver (PR), split into low (DC) and high (AC) frequency signals and digitised with two data acquisition cards (DAQ L: PCI-6251, DAQ H: PCI-5142, National Instruments, UK).

Purpose	Model	Mode	Wavelength (nm)	Energy
Ultrasound generation for MWCNT/PDMS composite	SPOT-10-500-1064, Elforlight, UK	Pulsed (2 ns)	1064	10 μJ
Ultrasound/Photoacoustic generation for CV & AuNP – PDMS composites	Spitlight 600, Innolas, UK	Pulsed (7 ns)	532 (ultrasound) 1210 (photoacoustic)	21 μJ (CV-PDMS ultrasound) 76 μJ (AuNP-PDMS ultrasound) 116 μJ (photoacoustic)
Interrogation of ultrasound receiver	Tunics T100S CL, Yenista Optics France	Continuous wave	1500-1600	1 mW

Table 1: Specifications of lasers used for ultrasound transmission and reception

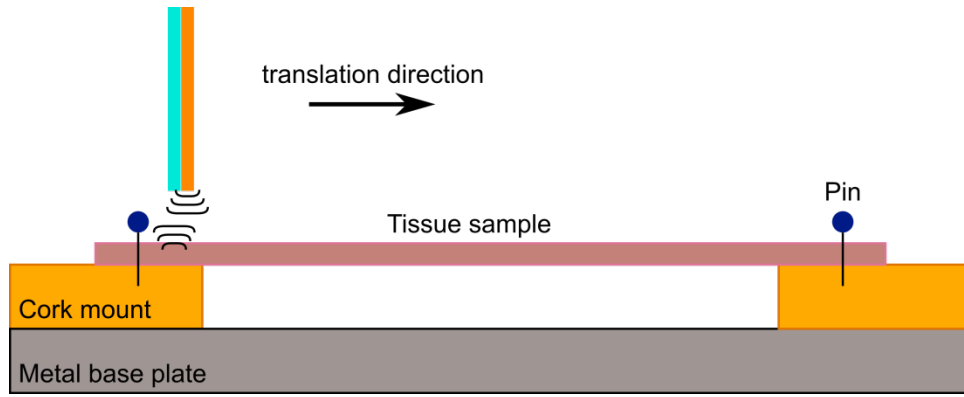


Figure 3: Schematic of image acquisition for all-optical ultrasound and all-optical photoacoustic imaging. Tissue was pinned to a cork mount and the imaging probe was scanned laterally above the tissue surface.

Processing of photoacoustic and ultrasound signals comprised background signal removal, time-gain compensation and image synthesis. For both modalities, the background signal originated predominantly from ultrasound transmission directly between the composite coating and the receiver. In the photoacoustic case, this was due to the small absorption of 1210 nm in the coatings, leading to ultrasound generation. The signal was removed using a general linear model, as described previously^[2]. For the photoacoustic image, residual ultrasound signals which were reflected by the imaging target were removed by scaling and subtracting the pure ultrasound image from the photoacoustic image. Subsequently, the first 1.5 μ s were tapered to suppress direct cross-talk between the source and the receiver fibres using a gain factor^[3]:

$$g(i) = \left[\frac{\min(i, i_{\max})}{i_{\max}} \right]^{\gamma}$$

where i was the sample index of the signal ($i = 1, 2, \dots$). The parameters i_{\max} and γ were chosen empirically to be 150 and 2.5, respectively. After time-gain compensation, high pass filtering (Butterworth, 4th order, 2.5 MHz) was performed, followed by low pass filtering (Butterworth, 4th order, 25 MHz (ultrasound), 15 MHz (photoacoustic)). Image synthesis comprised concatenation of the processed signals from different locations, followed by reconstruction with a k-space method with the assumption that optical transmission, ultrasound transmission, and ultrasound reception were omnidirectional^[2] and that transmission and reception occur in the same spatial location. Additionally, the speed of sound was assumed to be constant throughout the imaging volume. For both modalities, image synthesis was followed by envelope detection with the Hilbert transform and subsequent log transformation.

4 All-Optical Ultrasound and All-Optical Photoacoustic Images

Figures 4 and 5 show the individual ultrasound and photoacoustic images of *ex vivo* swine abdominal tissue and diseased human aorta acquired prior to overlaying them. The ultrasound images of the tissue samples show bright regions and these correspond to the locations at which photoacoustic signal is present. In Figure 4 (g) the fatty regions are clearly visible on the photograph and correspond well to both the ultrasound and photoacoustic images. In Figure 5 (g) a region of plaque is visible central to the section (red arrow), with the distinct yellow coloration associated with fat.

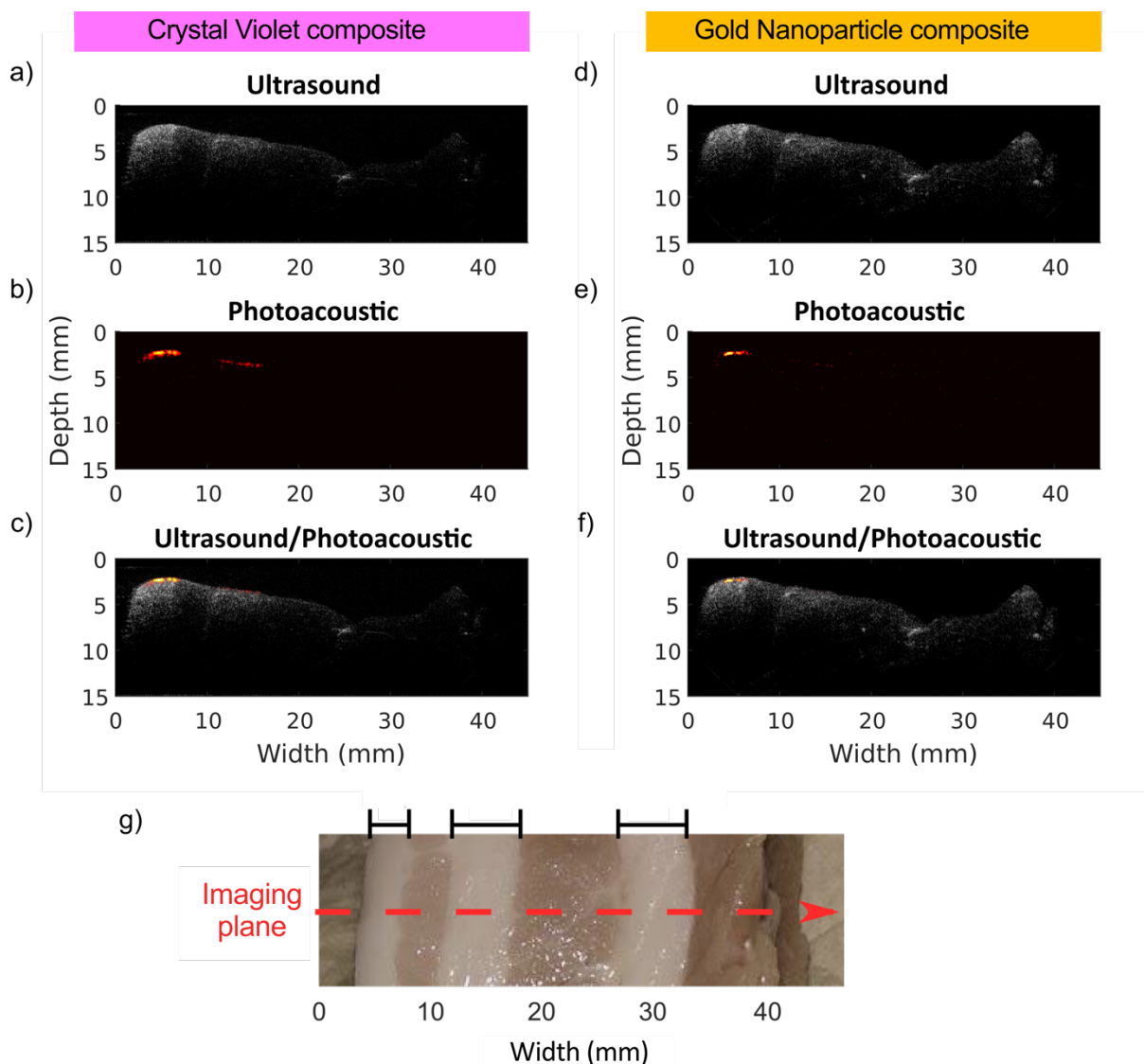


Figure 4: (a) Ultrasound (35 dB dynamic range), (b) photoacoustic (30 dB dynamic range) and (c) combined ultrasound/photoacoustic images of *ex vivo* swine abdominal tissue acquired using a CV-PDMS composite. (d) ultrasound (30 dB dynamic range), (e) photoacoustic (20 dB dynamic range) and (f) combined ultrasound/photoacoustic images of *ex vivo* swine abdominal tissue acquired using a AuNP-PDMS composite. (g) Photograph of the imaged *ex vivo* swine abdominal tissue, in which fatty regions (black bars) were interspersed with muscle.

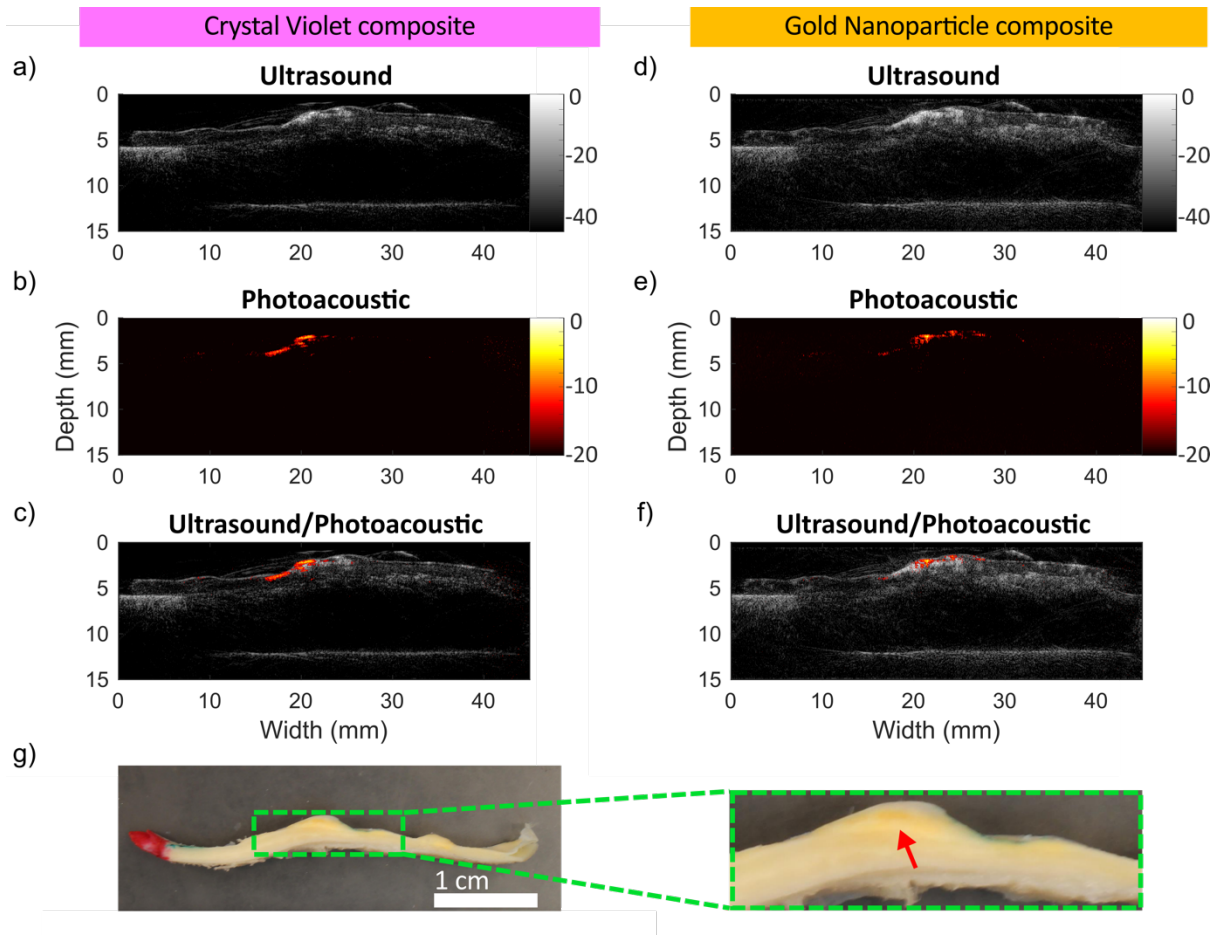


Figure 5: (a) Ultrasound (45 dB dynamic range), (b) photoacoustic (20 dB dynamic range) and (c) combined ultrasound/photoacoustic images of an *ex vivo* diseased human aorta section acquired using a Crystal Violet composite. (d) Ultrasound (45 dB dynamic range), (e) photoacoustic (20 dB dynamic range) and (f) combined ultrasound/photoacoustic images of an *ex vivo* diseased human aorta section acquired using a AuNP composite. (g) Photograph of aorta section prior to histology, the red marker indicates the proximal end. The red arrow corresponds to regions of plaque.

5 Histology of Human Aorta Sample

The histology of the human aorta section (Figure 6, 7) showed clearly the presence of a lipid rich plaque in the centre of the section. There was slight intimal thickening on the right-hand-side of the aorta, whilst the left-hand-side was healthy. Post-fixation with osmium tetroxide confirmed the presence fat that is evident as black regions within the plaque.

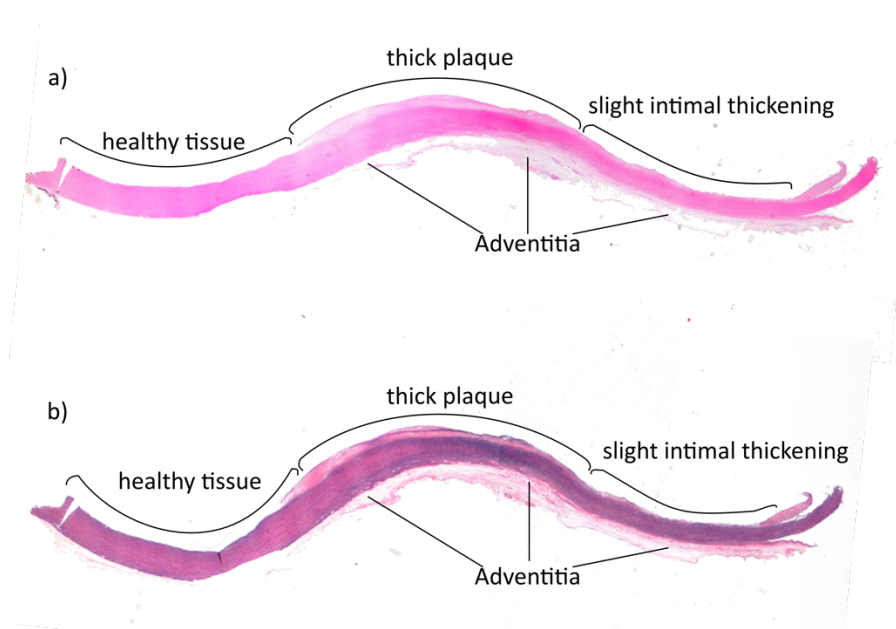


Figure 6: Histological sections through the ultrasound/photoacoustic imaging plane of the human aorta sample. Top: Haematoxylin and Eosin stain. Bottom: Elastic van Gieson stain.

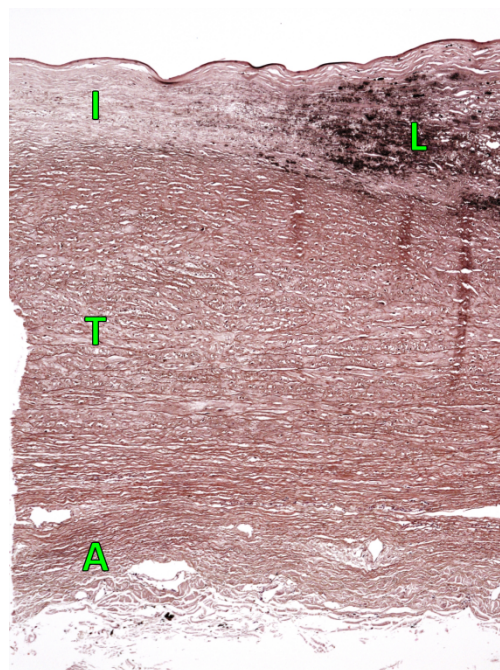


Figure 7: Histological cross-section (osmium tetroxide stain) of the imaged human aorta tissue. A lipid pool (L; black features) was apparent in the intima above the tunica media (T) and adventitia (A).

6 Bibliography

- [1] E. Z. Zhang, P. C. Beard, In *Proc. of SPIE, Photons Plus Ultrasound: Imaging and Sensing*; Oraevsky, A. A.; Wang, L. V., Eds.; 2015; Vol. 9323, p. 932311.
- [2] R. J. Colchester, E. Z. Zhang, C. A. Mosse, P. C. Beard, I. Papakonstantinou, A. E. Desjardins, *Biomed. Opt. Express* **2015**, *6*, 1502.
- [3] M. C. Finlay, C. A. Mosse, R. J. Colchester, S. Noimark, E. Z. Zhang, S. Ourselin, P. C. Beard, R. J. Schilling, I. P. Parkin, I. Papakonstantinou, A. E. Desjardins, *Light Sci. Appl.* **2017**, *In Press*.